CHAPTER IV

RESULTS AND DISCUSSION

In this chapter, the experimental results and discussion are deliberated for effect of the starting materials and process variables on the properties of specimen obtained in each preparation stage.

4.1 Characterization of alumina powder as raw material

The particle size distribution of commercially available alumina powder (TM-DAR) employed as raw material is demonstrated in Figure 4.1. The size of alumina powder is in the range of 47.5 to 3000 nm. Its average particle size (d_{50}) basis determined cumulative volume as shown in Figure 4.1(b).

As a result, the usage of nanopowder as the starting material is an important factor. It not only results in smaller grain size within the sintered sample but also decreases the pore between particles within green compact. Both of these characteristics lead to the improvement of light transmission due to multilevel scattering inside the specimen (Apetz and Bruggen, 2003).

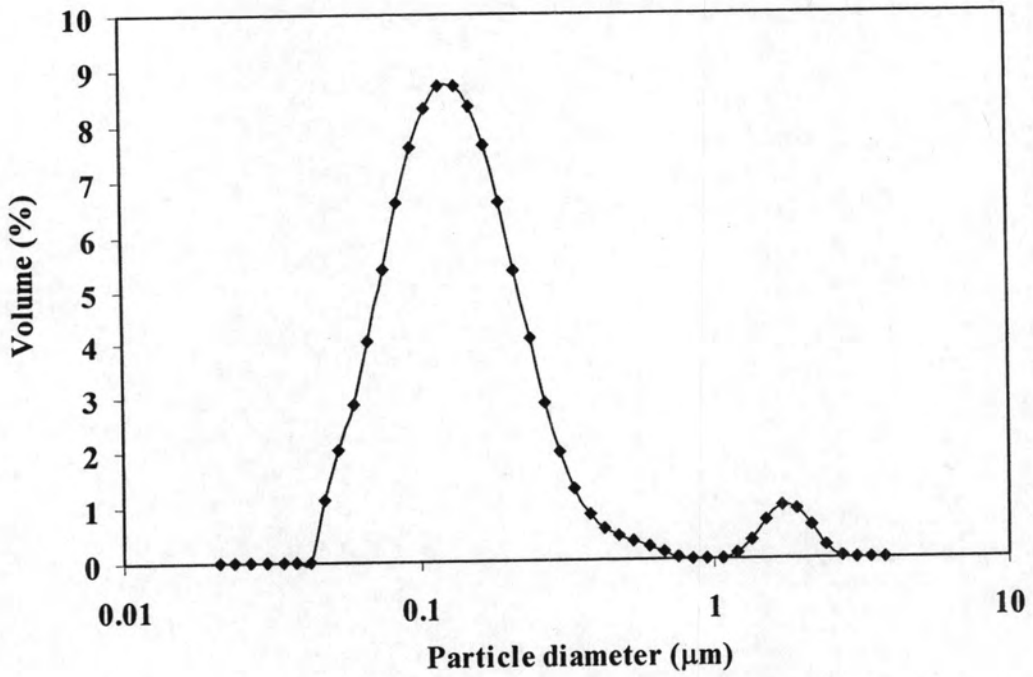

(a)

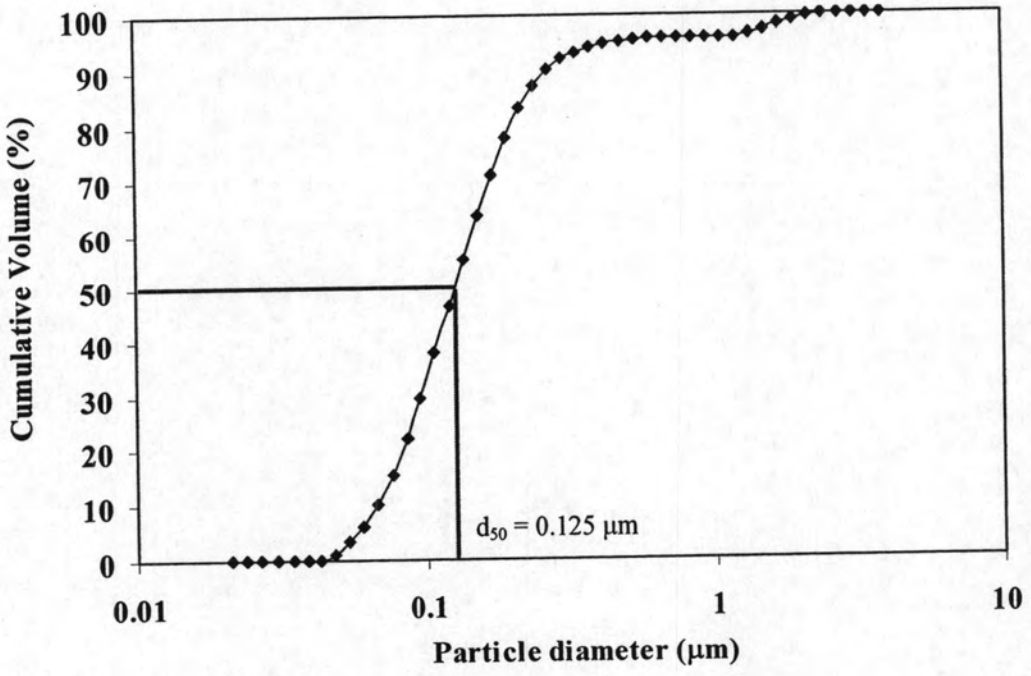

(b)

Figure 4.1 Particle size distribution of TM-DAR alumina powder (a) volume (%) by frequency (b) cumulative volume (%)

4.2 Effect of organic binder on alumina suspension suitable for slip casting method

Normally, strength of a green body must be adequate to permit its removal from mold, drying and handling prior to the firing operation. Binder is an important additive used to aid the forming of green body by casting method. Therefore, the addition of PVA binder as well-known additive in alumina suspension was examined at the beginning of this work.

Composition of each constituent in alumina suspension prepared in this research was investigated. PVA binder in the range of 0-1.5 wt% was added to the mixture with the optimal NH_4^+-PMAA dispersant concentration of 1.18, 1.25 and 1.5 wt% (referred to Areeraksakul, 2005) with respect to the alumina content of 70, 75 and 80 wt%. All compositions are summarized in Table 4.1. It should be note that the amount of dispersant and binder use in this research is expressed on a dry weight of the powder basis.

Table 4.1 The composition of alumina suspensions

Sample	Composition (wt%)			
	Alumina	Water	Dispersant*	Binder*
A	70	30	1.18	0-1.5
B	75	25	1.25	0-0.5
C	80	20	1.5	0-0.1

*Based on dry alumina powder weight

4.2.1 Effect of spindle speed on the viscosity of the alumina suspensions

According to the experimental result shown in Figure 4.2-4.4, an apparent viscosity of alumina slurry at the each PVA binder concentration with 70, 75 and 80 wt% solid content was inversely proportional to spindle speed but it became constant at high spindle speed. It can be clearly seen that the alumina suspensions with and without added PVA binder exhibit non-Newtonian fluid with pseudo plastic behavior.

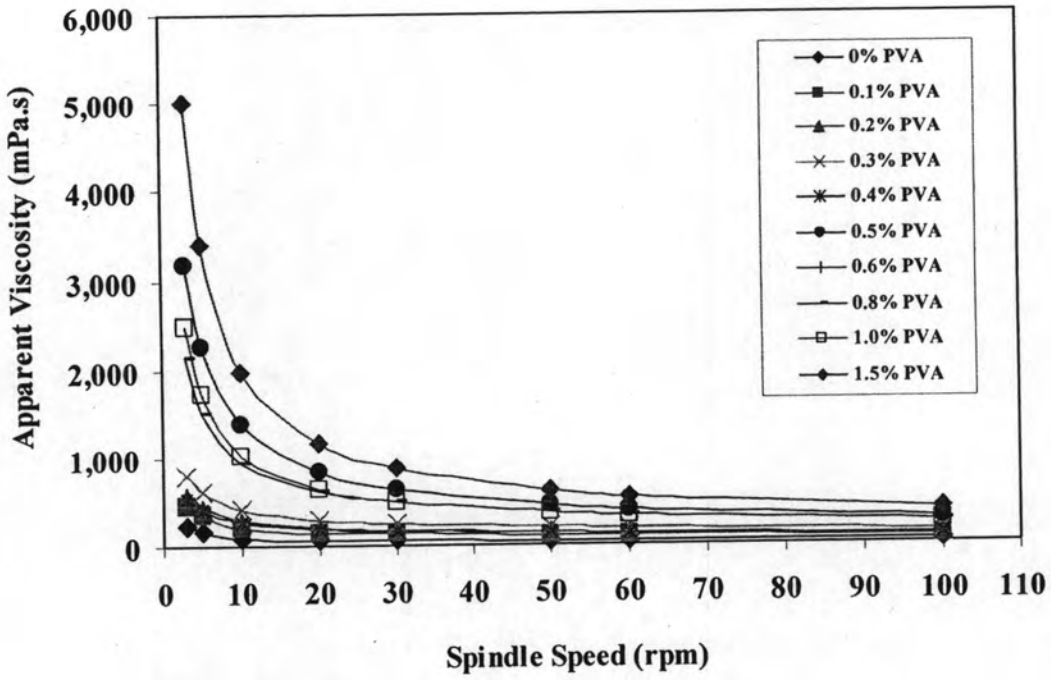

Figure 4.2 Effect of spindle speed on the apparent viscosity of the alumina suspensions with 70 wt% solid content and 1.18 wt% dispersant at various binder concentrations

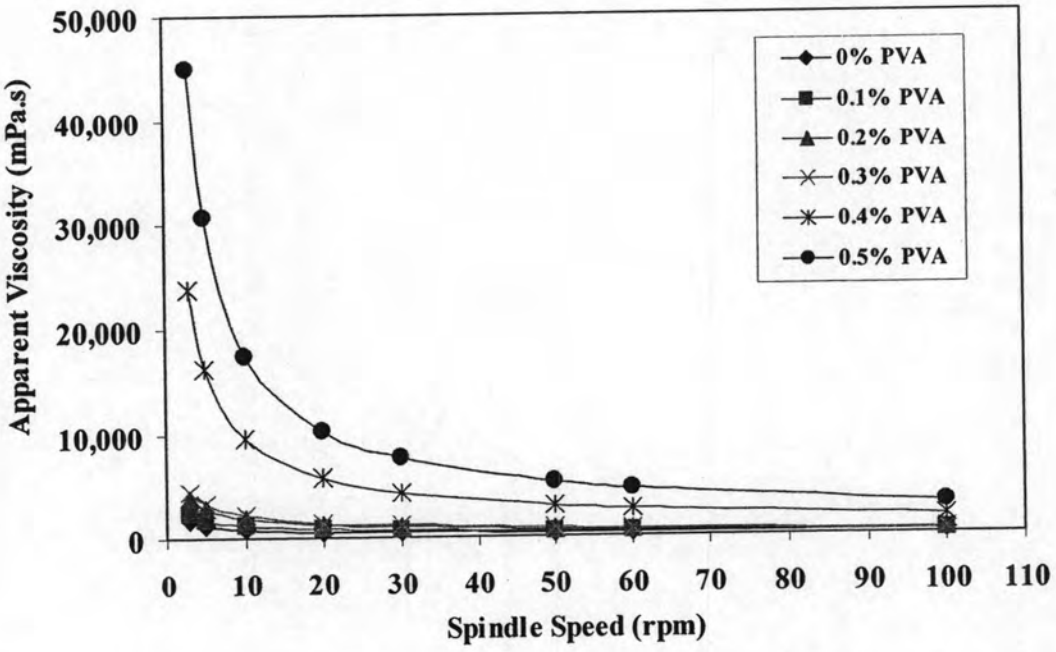

Figure 4.3 Effect of spindle speed on the apparent viscosity of the alumina suspensions with 75 wt% solid content and 1.25 wt% dispersant at various binder concentrations

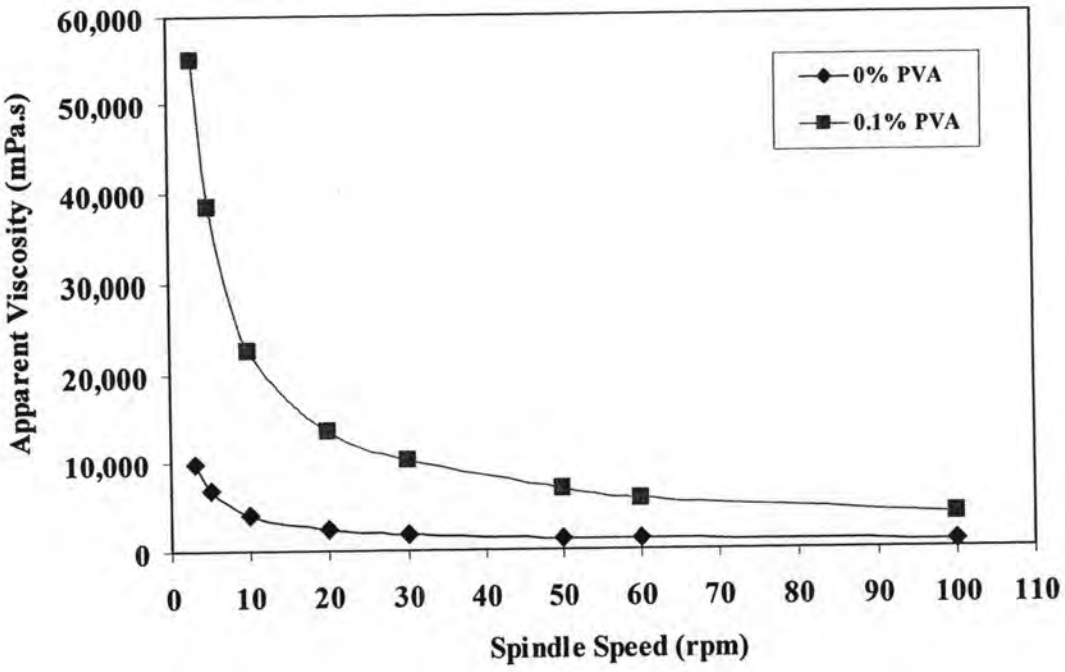

Figure 4.4 Effect of spindle speed on the apparent viscosity of the alumina suspensions with 80 wt% solid content and 1.5 wt% dispersant at various binder concentrations

4.2.2 Effect of organic binder concentration on the viscosity of the alumina suspensions

Effect of the binder concentration with 70, 75 and 80 wt% solid content on the apparent viscosity was illustrated in Figure 4.5. For 70 wt% alumina content, the apparent viscosity gradually increased from 39 to 382 mPa.s as the increased binder content was increased. For 75 wt% alumina content, the slurry viscosity gradually increased with the increased binder content up to 0.3 wt% (490 mPa.s), and then drastically increased to 1900 mPa.s when the 0.4 wt% binder was added. However, at 80 wt% alumina content, the viscosity drastically increased from 787 mPa.s to 3867 mPa.s by introducing only 0.1 wt% binder content. It might be attributable that the binder molecules adsorbed on surface of alumina particles could form weak bridging forces among alumina particles, resulting in flocculation and more viscous slurry.

Furthermore, the amount of solid content in alumina suspension is significant on the apparent viscosity. Constantly the PVA binder concentration, the

slurry viscosity increased at high alumina content. It can be explained by the more particle-particle attraction which will increase the viscosity by increasing the force required to move one particle past another.

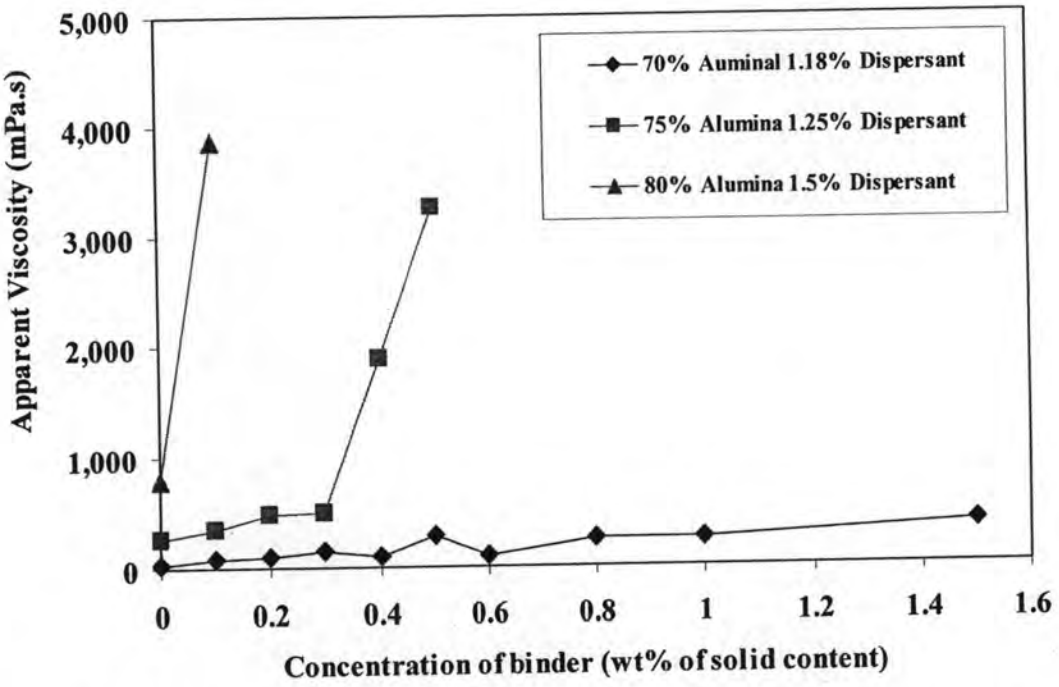

Figure 4.5 Effect of PVA binder concentration and solid content on alumina slurry viscosity with a rotational speed of 100 rpm

Practically, alumina slurries with a viscosity over 2000 mPa.s were too viscous for slip casting it in gypsum molds. However, the purpose of this research is to prepare the high density of green body which produced from the high solid content of slurry. It is expected to employ alumina slurry with solid content as high as possible. In contrast, the high solid content of slurry (80 wt% alumina content) exhibited too high viscosity. When a continuous network of touching particles spans the bulk volume of the suspension, suspended particles are no longer free to move with in the suspension (Dinger, 2002). It is the reason why 80 wt% alumina content was not suitable for slip casting.

Therefore, the available content of PVA binder employed for further process should be in the range of 0 - 0.4 wt% and 1.25 wt% dispersant for 75 wt% solid content.

4.3 Effect of organic binder on alumina green body

Accordingly, the composition of the suitable alumina slurries for slip casting was at 75 wt% of alumina content and 1.25 wt% dispersant with the binder concentration not exceeding 0.4 wt%. As a result, alumina slurries with suitable viscosity were prepared in the circular pellet shape, cylindrical shape and alphabet shape. The addition of PVA binder on the green bodies was further observed.

4.3.1 Strength of the alumina green body

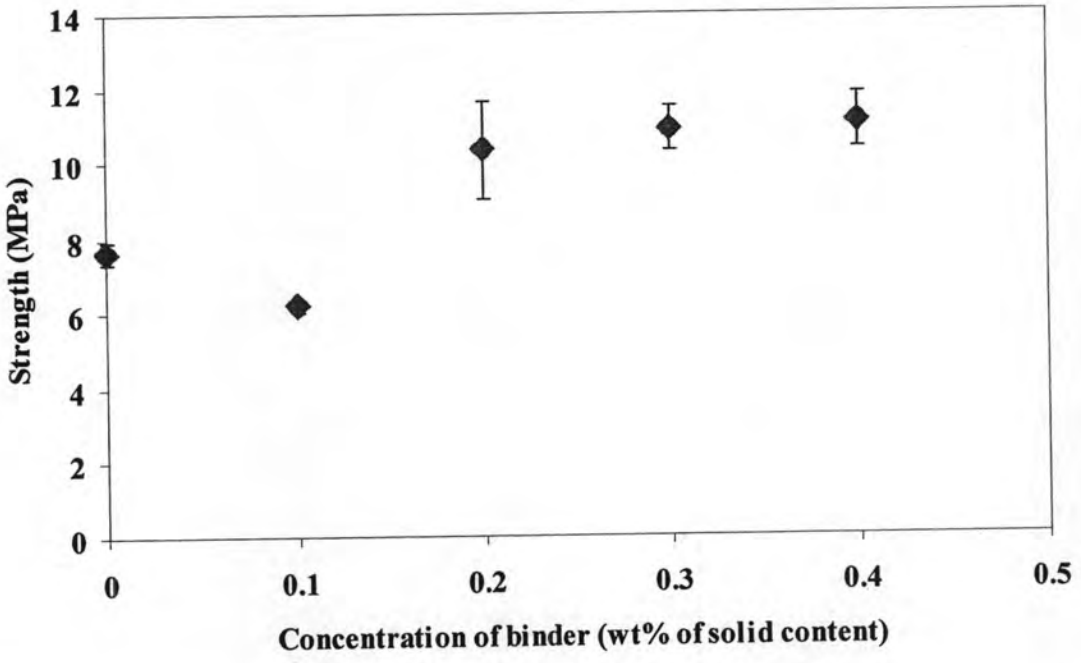

Figure 4.6 Effect of PVA binder concentration in slurries with 75 wt% solid content and 1.25 wt% dispersant on the strength of alumina green body

From Figure 4.6, strength of the alumina green bodies depended on the PVA binder concentration. It was found that the average strength decreased from 7.6 to 6.2 MPa when the PVA binder adding up to 0.1 wt%. Meanwhile, the green body with up to 0.2 wt% binder had the increasing average strength from 10.3 to 11.1 MPa. This result suggested that the addition of organic binder resulted in the increasing of the green strength. However, the low green strength of 0.1 wt% binder was caused by an inhomogeneous distribution of binder for example the bubbles occurred in the specimen.

Satapathy (2000) explained the benefit of using a high-green-strength binder. The low binder level would provide enough green strength for process requirements. Our experimental results are in good agreement with this reported result. Consequently, the PVA binder concentration of 0.2 wt% is suitable for handling the desired shape.

4.3.2 Appearance of the alumina green body

Appearance of the green bodies was shown in Figure 4.7. Prepared specimens are the pellet shape with diameter of 30 mm and thickness of 4 mm and alphabet shape of T, C and U. The color of alumina green bodies is as white as the raw material.

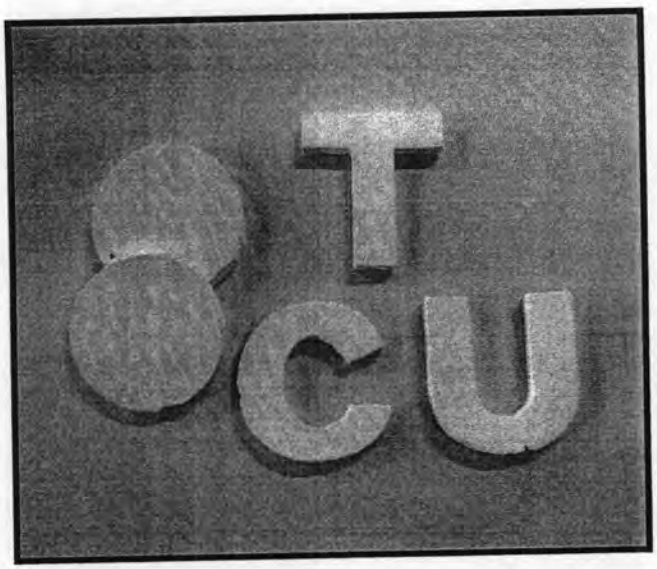

Figure 4.7 Alumina green bodies in various shapes

4.4 Effect of organic binder on alumina calcined body

The green bodies were fired at 800°C for 2 h in air atmosphere with heating rate of 10°C/min so as to burn out the organic binder. The effect of PVA binder addition on the calcined bodies was investigated.

4.4.1 Density of the alumina calcined body

The calcined alumina specimens with PVA content of 0-0.4 wt% have the relative density higher than 55% as shown in Figure 4.8. It could experimentally be observed the relative density of prepared specimen decreased from 61% to 57% with the increasing PVA concentration from 0 to 0.4 wt%. The drop of relative density is attributed to an increase in porosity within the specimens due to the decomposition of PVA at the calcining temperature of 800°C.

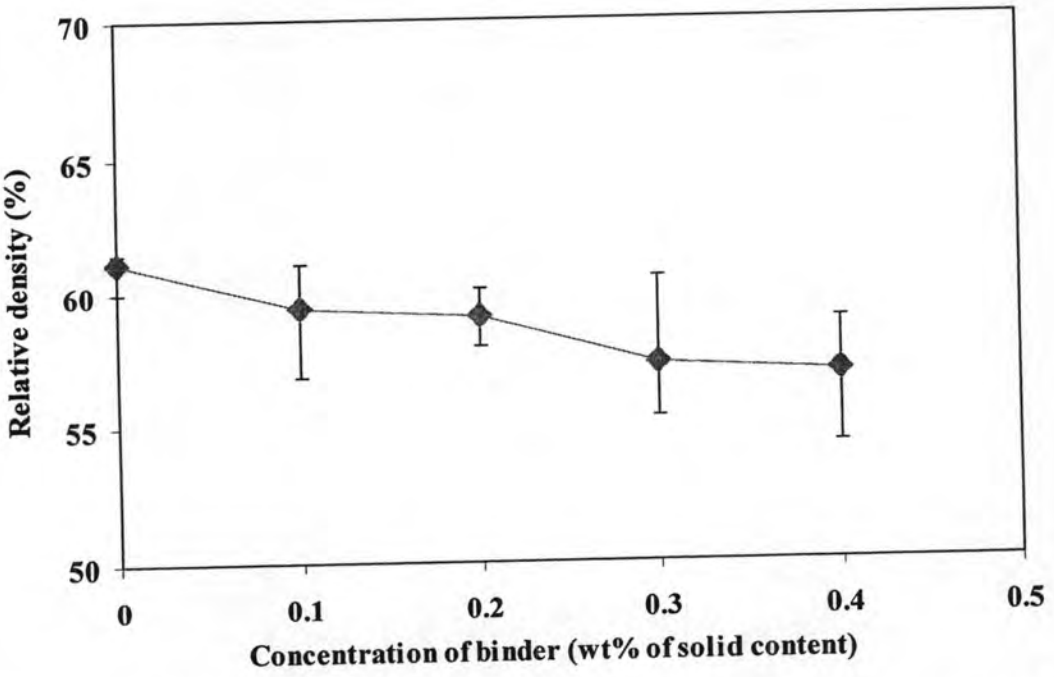

Figure 4.8 Effect of PVA binder concentration on the relative density of calcined body with 75 wt% alumina content

Based on the results of the green body strength and calcined density, the optimal amount of PVA binder is controlled to not exceed 0.2 wt%. Alumina specimens with the concentration of PVA binder in the range of 0-0.2 wt% could exhibit a high density of calcined bodies and the sufficient strength to the green bodies in desired shape without the breaking or damage before and during sintering. Consequently, calcined bodies with high strength could be prepared.

4.4.2 Morphology of the alumina calcined body

Figure 4.9 illustrates typical microscopic images of alumina grains within the green body and calcined body specimens. The compact body of alumina powder before calcination contains smooth surface and uniform distribution of alumina seeds as shown as in Figure 4.9 (a). Inversely, after calcination a slice increase in the grain size but a small increase in the specimen porosity within the calcined body could be observed in Figure 4.9 (b).

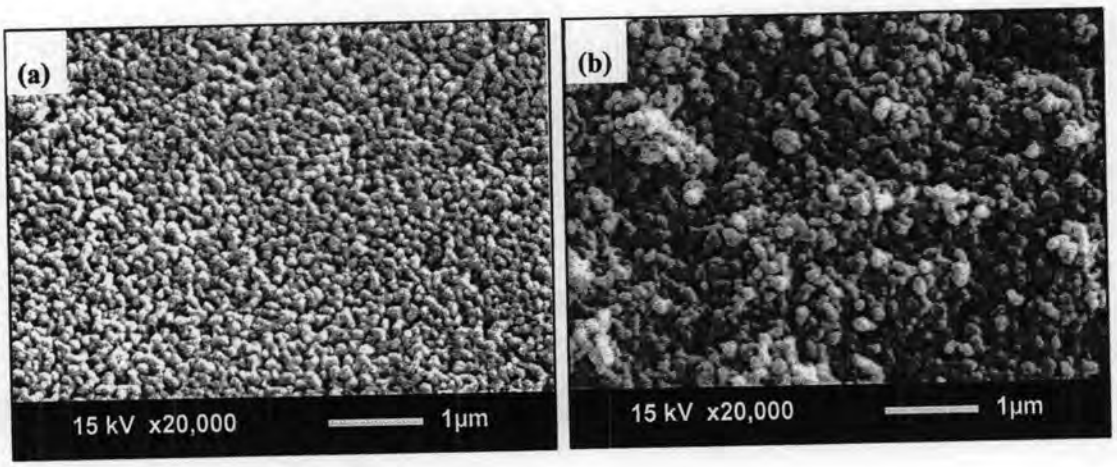

Figure 4.9 SEM micrograph of (a) alumina green body and (b) calcined body with 75 wt% alumina content, 1.25 wt% NH_4^+-PMAA dispersant and 0.2 wt% PVA

4.5 Effect of acid treatment on alumina calcined body

Before sintering, the calcined bodies should be treated with acid in order to eliminate the impurities such as $CaSO_4$ from gypsum mold. In the acid treatment, the specimens were immersed in 1 M HCl solution for 1 h. The energy dispersive spectrometer (EDS) analysis was used to characterize the calcined bodies before and after acid treatment as illustrated in Figure 4.10. It was found that the calcined specimens before acid treatment were contaminated with Ca^{2+} as 1.16 wt% and disappeared after the treatment.

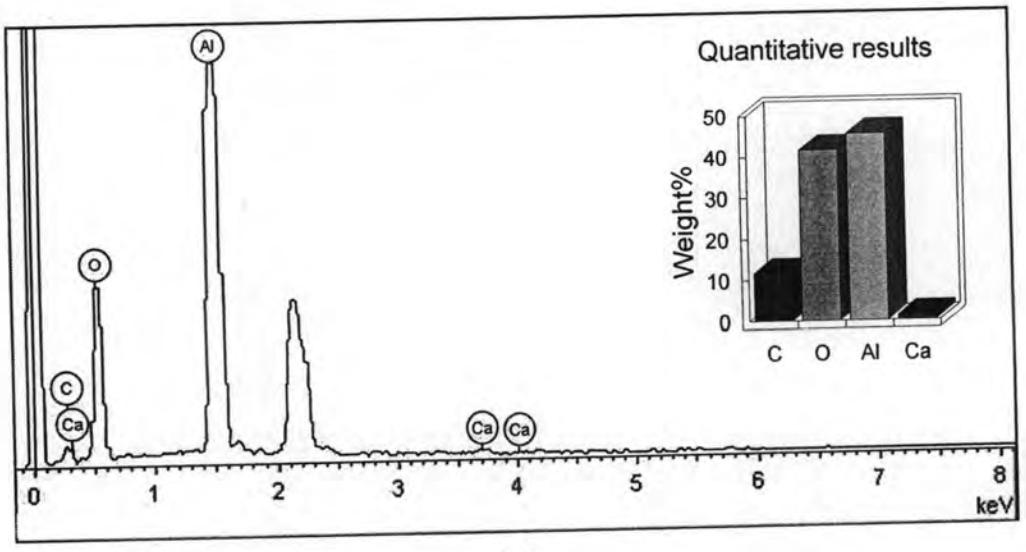

(a)

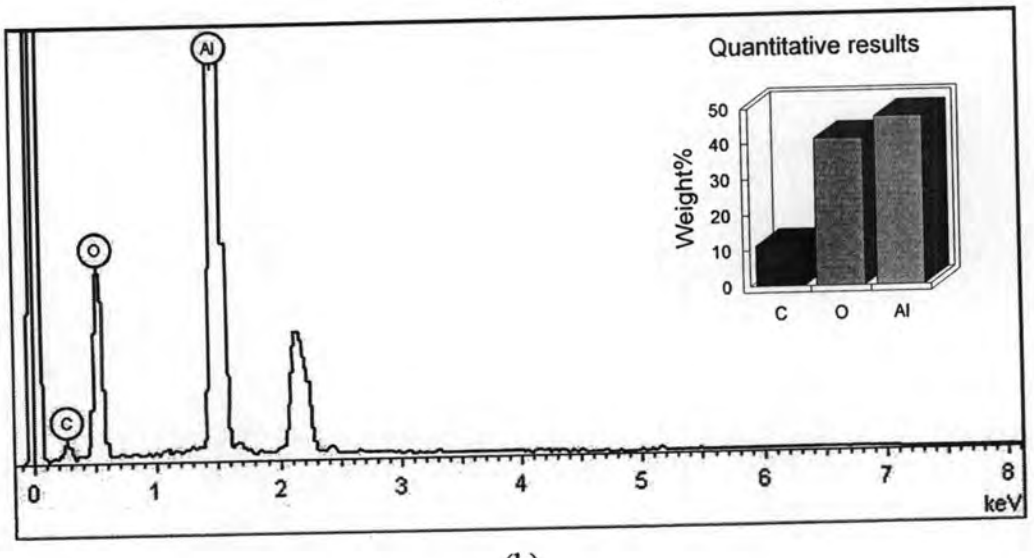

(b)

Figure 4.10 EDS analysis of calcained body of (a) before and (b) after acid treatment

4.6 Effect of sintering type, temperature, soaking time and sintering technique in pre sintering process on the alumina sintered body

From the previous experiment, the results of viscosity of slurry, green strength and calcined density were obtained to justify what kind of specimen should conduct to further process. The specimens with 75 wt% alumina content, 1.25 wt% dispersant and not over 0.2 wt% binder were selected to investigate for pre sintering conditions. The density, shrinkage and morphology of sintered specimen was examined in the pre-sintering conditions in order to obtain the full density and the small grain size leads to provided transparent alumina samples.

4.6.1 Density of the alumina sintered body

In the pre-sintering step, calcined specimens were subject to a temperature in a range of 1250–1400°C with a heating rate of 10°C/min. Then the specimens were kept at the sintering temperature for a certain soaking time before cooled down with the cooling rate of 10°C/min. The relative density of sintered specimens is compared in Figure 4.11. By atmosphere sintering at 1300-1400°C with suddenly cooling (soaking time = 0 h), an increase in the relative density of sintered specimens (▲) from 77 to 97% could be achieved without soaking. Besides, the relative density of specimens sintered under atmospheric condition (■) increased from 96 to 100% after sintering at 1250-1350°C with soaking time of 2 h. In general, it is supposed that alumina specimens sintered under vacuum condition would have relative density higher than that of atmospheric sintered specimens. However, the density of specimens sintered in a vacuum furnace (◆) is about 5% lower than that of atmospheric sintered specimens. This is attributable to the existence of graphite heating elements in the vacuum furnace, resulting in a reducing condition of oxygen with very low partial pressure.

Considering Figure 4.12, the relative density of specimens sintered at 1350°C with different soaking time of 0 to 5 h was observed. The relative density increased from 91.6 to 99.9% with an increase in soaking time from 0 to 1 h. On the other hand, the specimen relative density was achieved 100% with soaking time of 2 h or longer. It has been clearly seen that the initiated soaking time provided the full density specimen was for 1 h at the temperature of 1350°C in atmosphere furnace.

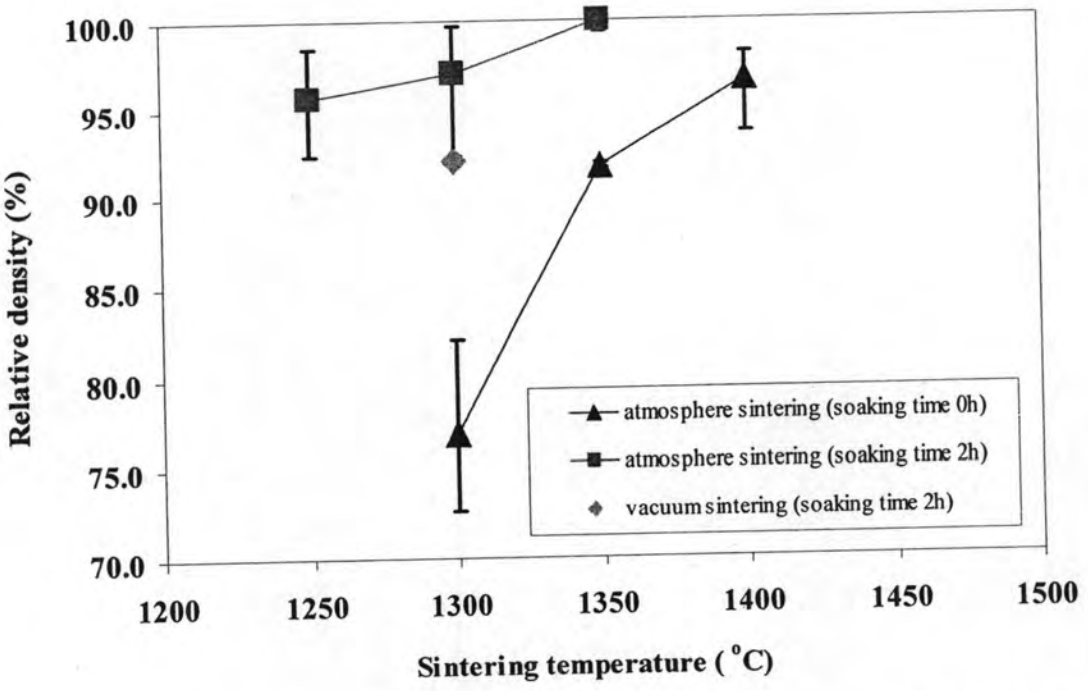

Figure 4.11 Relative density of specimens sintered in atmosphere and vacuum sintering at heating rate of 10°C/min and sintering temperature range of 1250 to 1400°C with different soaking time

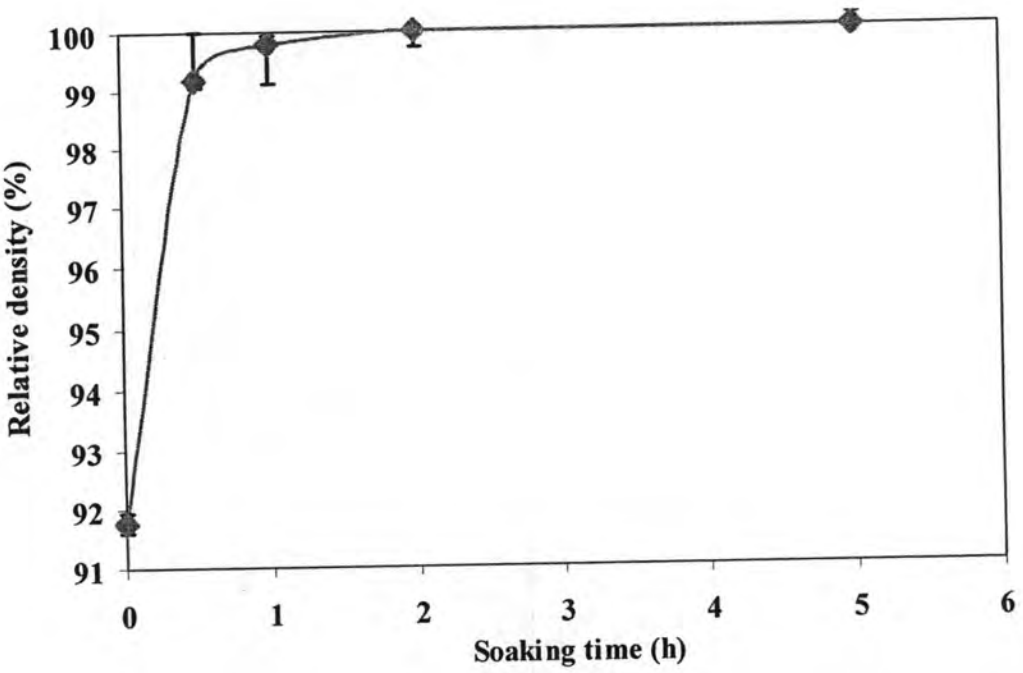

Figure 4.12 Relative density of specimens sintered in atmosphere furnace at the temperature of 1350°C and the heating rate of 10°C/min as a function of soaking time

4.6.2 Shrinkage of the alumina sintered body

As the sintered specimen with the desired shape, the shrinkage profile must be concerned. The shrinkage of specimen was examined by the measurement of the dimension in both before and after sintering by vernier caliper. The sintering type, temperature and soaking time on the linear shrinkage was exhibited in Figures 4.13 and 4.14. It was known that the linear shrinkage directed variation with the relative density because the densification mechanism in the sintering process could lead to the increasing shrinkage of calcined body to form the sintered body.

As could be observed in Figure 4.15, the linear shrinkage was insignificant with the shape of samples. The linear shrinkage was constant with various shapes.

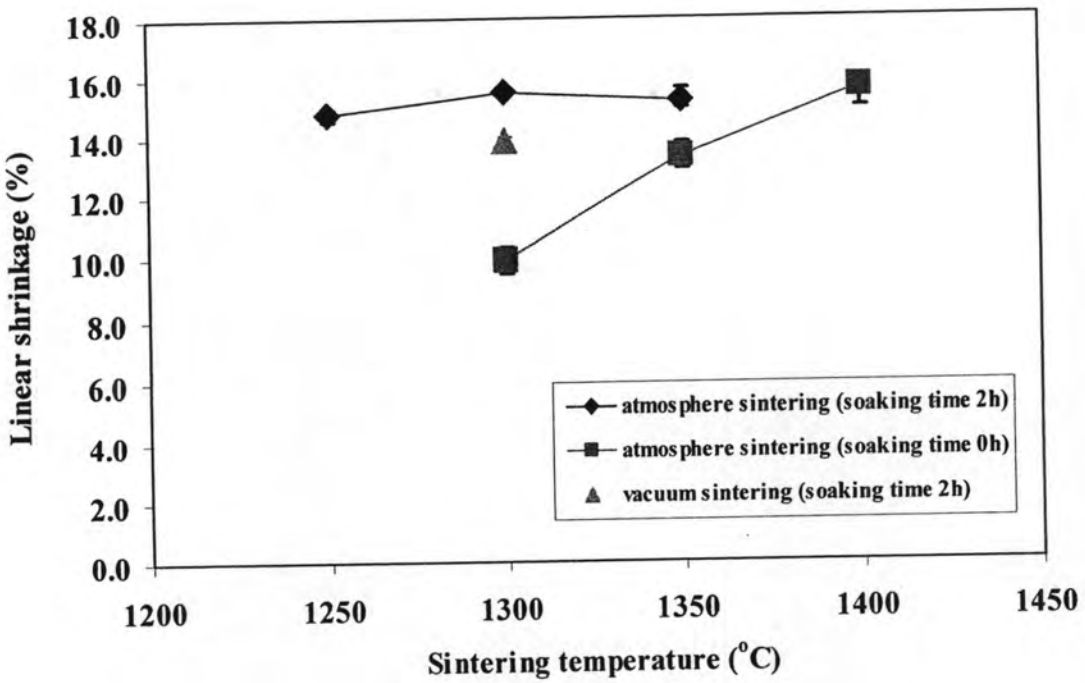

Figure 4.13 Linear shrinkage of specimens sintered in atmosphere and vacuum sintering at heating rate of 10°C/min and sintering temperature range of 1250 to 1400°C with different soaking time

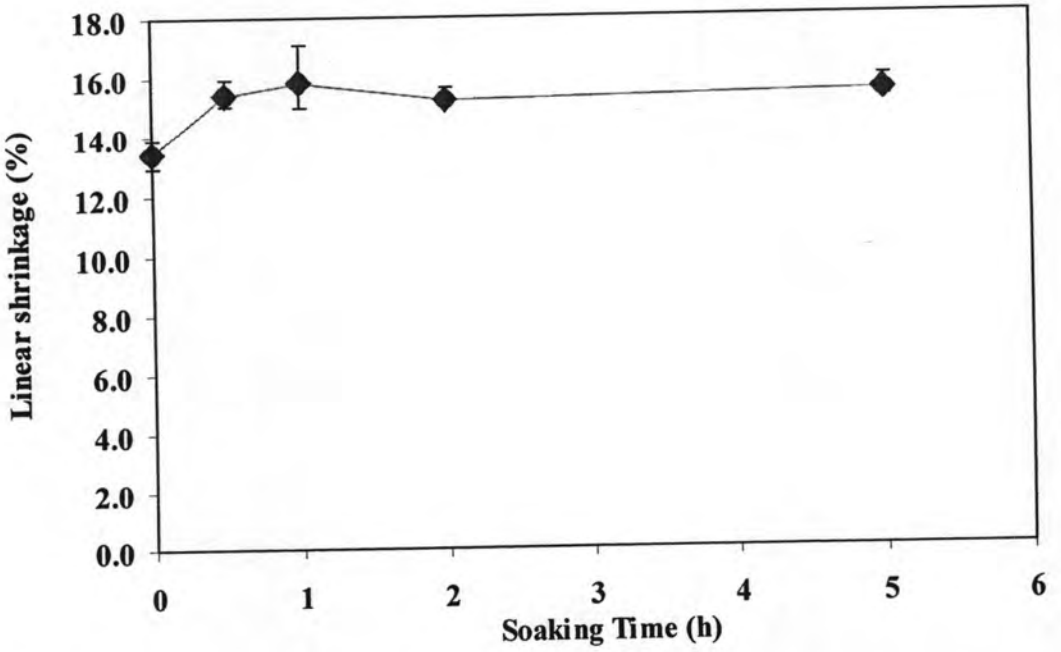

Figure 4.14 Linear shrinkage of specimens sintered in atmosphere furnace at the temperature of 1350°C and the heating rate of 10°C/min as a function of soaking time

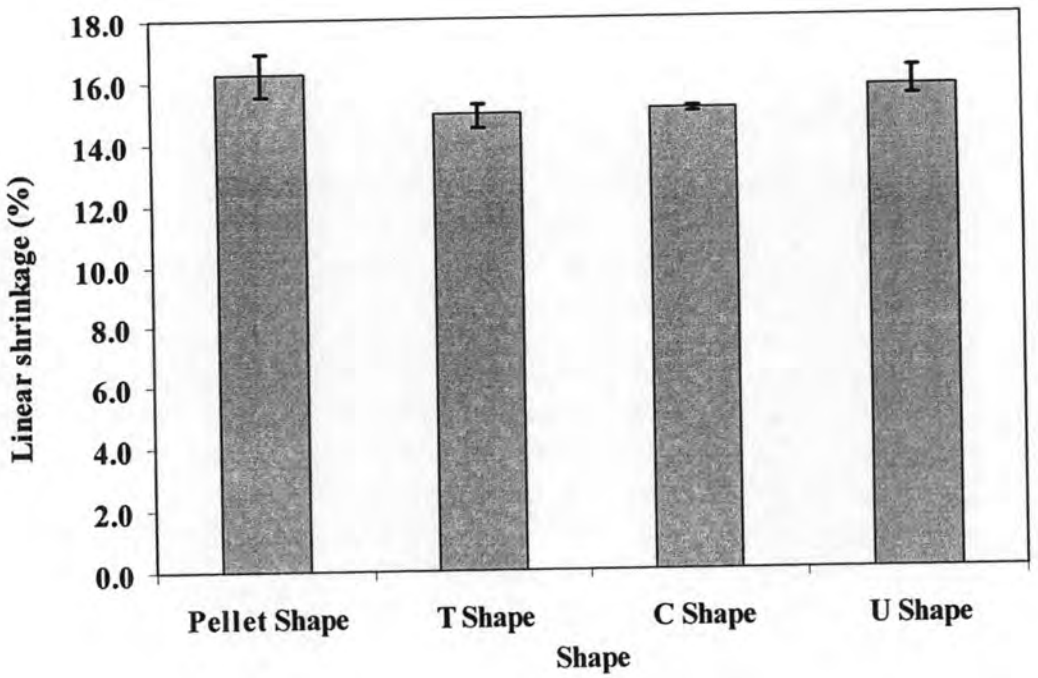

Figure 4.15 Linear shrinkage of specimens sintered in atmosphere furnace at temperature of 1300°C for 2 h as a function of shape

4.6.3 Microstructure and average grain size of the alumina sintered body

In this research, microstructure of sintered specimen was characterized by two methods which are the scanning electron microscope (SEM) and the atomic force microscope (AFM).

First, the effect of sintering type and soaking time on the average grain size and microstructure characterized by SEM was illustrated in Figures 4.16, 4.17 and 4.18, respectively. It was found that the grain size with pre-sintered in vacuum furnace at temperature of 1300°C for 2 h was smaller than that of 0.032 μm in atmosphere furnace at the same condition. Regarding to the soaking time factor, the grain size increased with the longer soaking time. Interestingly, the average grain size increased drastically with soaking time of 1 h to 2 h. It has been clearly explained that the grain growth mechanism immediately occurred after densification in sintering process.

According to the alumina ceramic which the high resistance property as an insulator, the morphology of alumina sample characterized by SEM was difficult to investigated. SEM evidence was obtained from introducing the electron beam onto the surface of sample and detecting signals with the electron that is suitable for conductive materials. Consequently, the characterization of microstructure by AFM is the new alternative of insulator material. From this reason, the morphology of sintered sample in this research was characterized by AFM.

As shown in Figure 4.19, the average grain size of specimens sintered at temperature in range of 1300 to 1400°C without soaking increased with the increase in sintering temperature. Meanwhile, the specimen sintered at temperature of 1250°C for 2 h was larger than that of the specimen sintered at temperature of 1300°C without soaking. The microstructure of sintered specimen was illustrated in Figure 4.20.

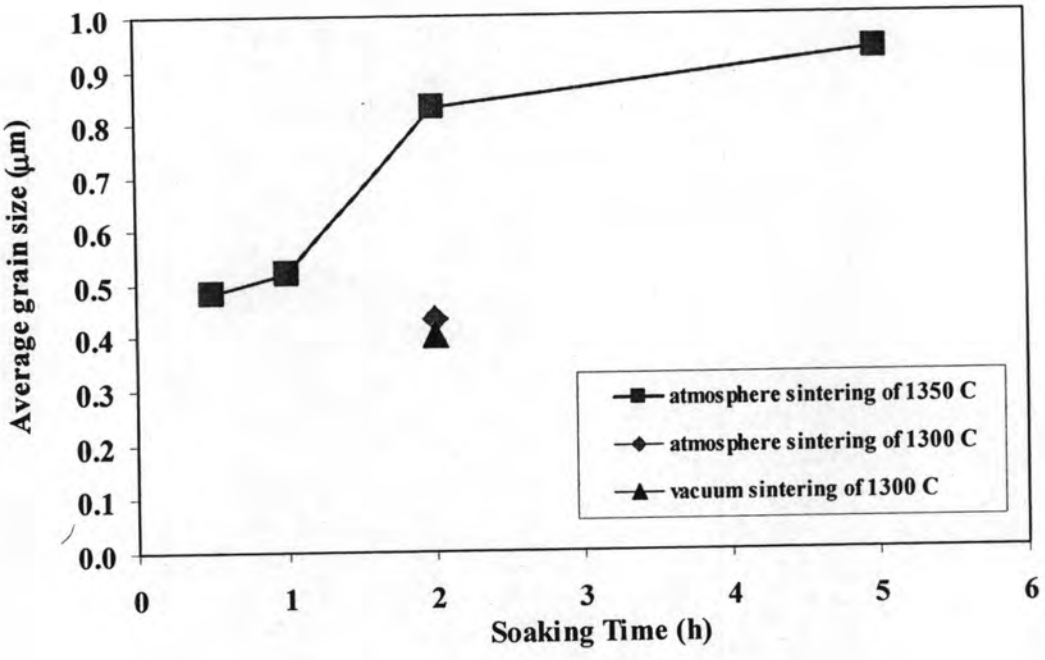

Figure 4.16 Grain size of specimens sintered in atmosphere and vacuum sintering at heating rate of 10°C/min and sintering temperature of 1300°C and 1350°C with different soaking time

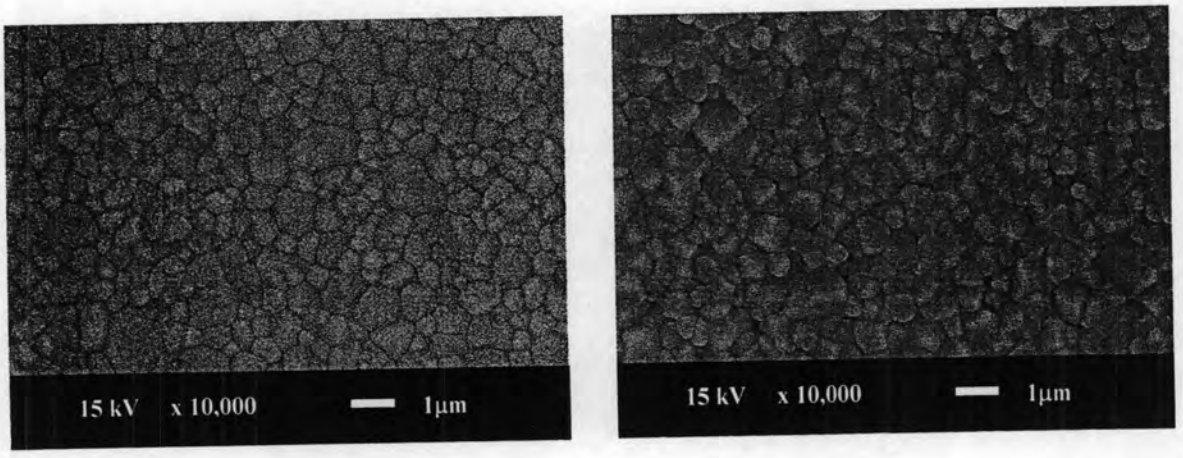

(a) (b)

Figure 4.17 SEM micrograph of alumina specimen sintered at 1300°C for 2 h at heating rate of 10°C/min in (a) atmosphere furnace (b) vacuum furnace

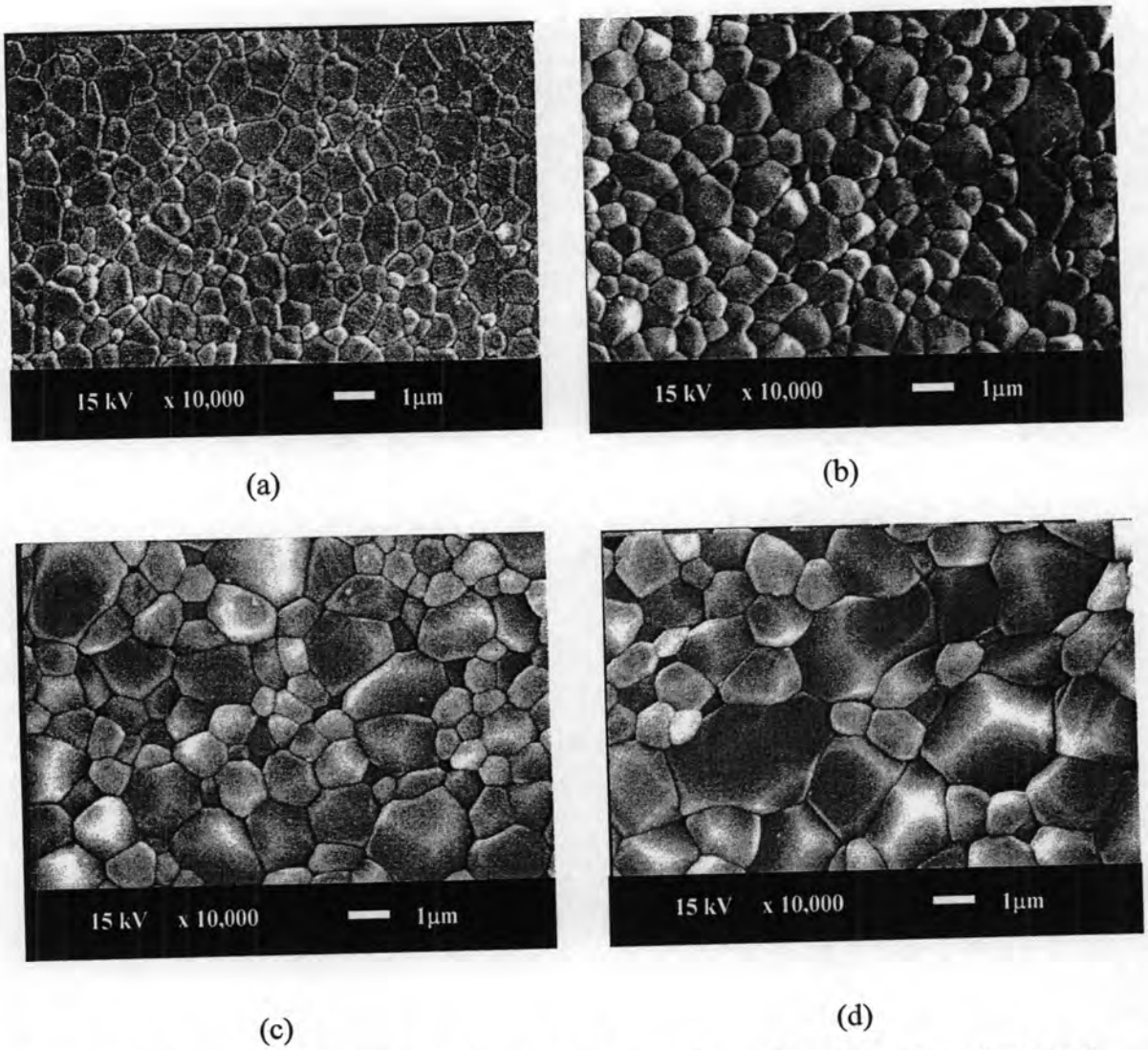

Figure 4.18 SEM micrograph of alumina specimen sintered in atmosphere furnace at 1350°C and heating rate of 10°C/min for (a) 0.5 h (b) 1 h (c) 2 h (d) 5 h

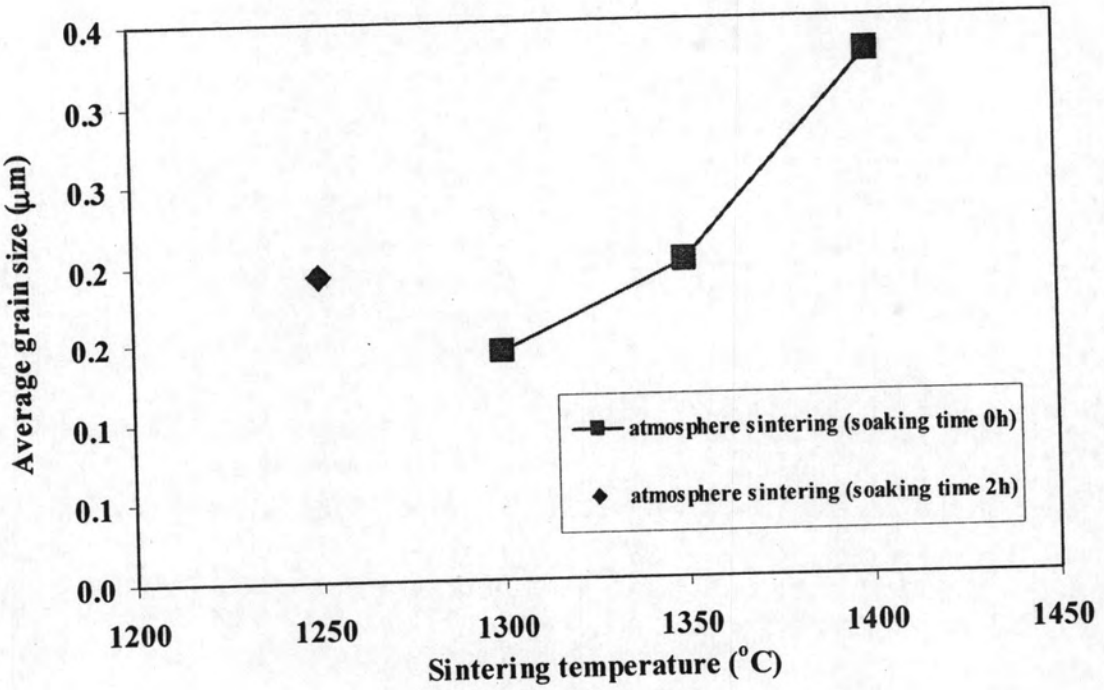

Figure 4.19 Grain size of specimens sintered in atmosphere at heating rate of 10°C/min and sintering temperature range of 1250 to 1400°C with different soaking time

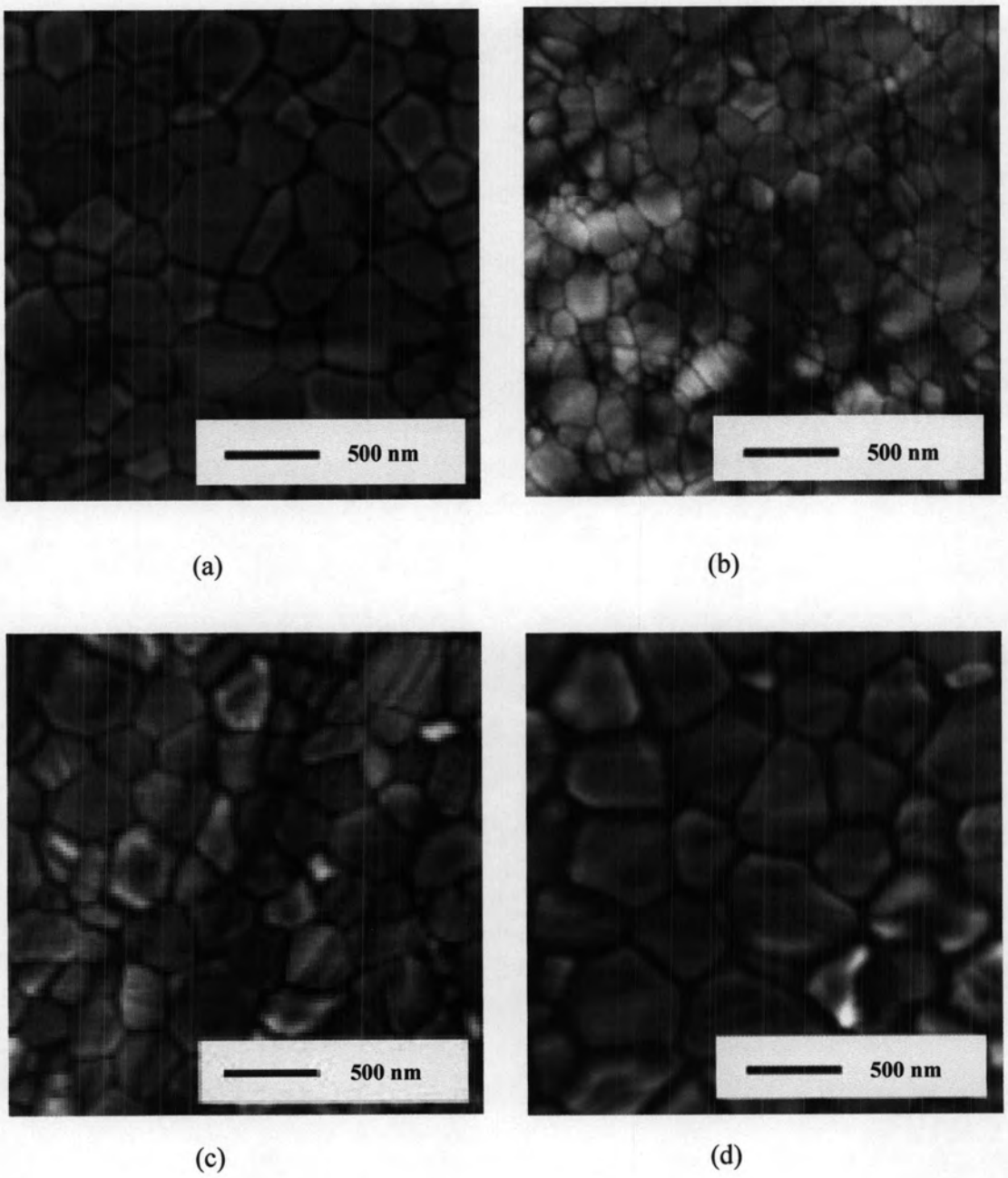

Figure 4.20 AFM micrograph of alumina specimen sintered in atmosphere furnace at heating rate of 10°C/min and temperature range of 1250 to 1400°C with different soaking time as followed (a) 1250°C 2 h (b) 1300°C 0 h (c) 1350°C 0 h (d) 1400°C 0 h

4.6.4 Appearance of the alumina sintered body

The appearance of the sintered bodies with normal pellet and alphabet shape was revealed by Figure 4.21. The color of alumina sintered bodies is still as white as the green body. However, some shrinkage took place, result in the size smaller than the green samples.

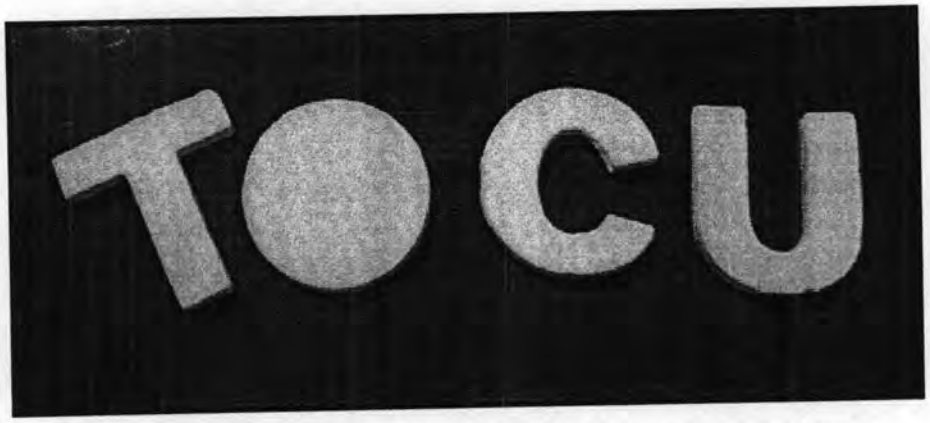

Figure 4.21 The alumina pre-sintered bodies in various shapes

4.6.5 Two-step sintering technique of the alumina sintered body

Generally, high temperature could result in rapid grain growth and enhance the densification of alumina ceramics, as also observed in Figure 4.16. Therefore, this research intentionally makes use of a two-step sintering to suppress the grain growth. With two-step sintering, green body specimens were first heated to a higher temperature to achieve an intermediate density, then they were cooled down and held at a lower temperature until it is full dense. The schematic of the two-step sintering was illustrated in Figure 4.22.

From the experimental result in Figure 4.22, it could seen that the grain size was a directly proportion to the relative density. The gain with the single-step sintered at 1400°C for 1h and the two-step sintered at 1400°C, and 1150°C for 5 h had different size of 0.421 and 0.377 μm, respectively. Meanwhile, the relative density with the two-step sintering more became the full dense than the single-step. It has

been clearly explained that the two-step sintering could provide the fabricated specimens with high density and the suppression of the grain growth.

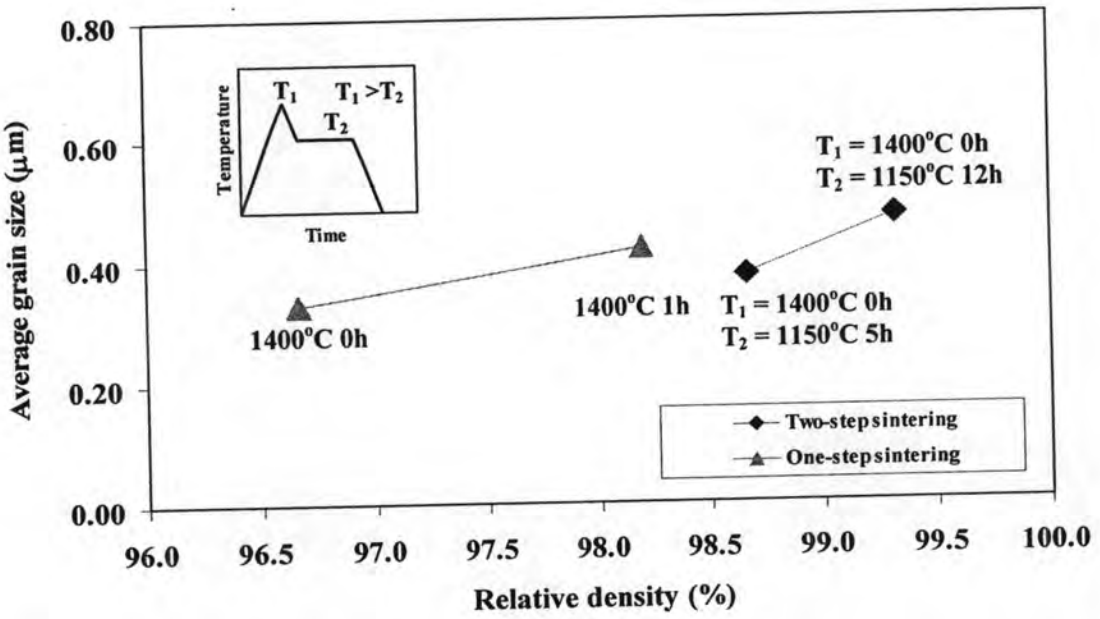

Figure 4.22 Relation between grain size and relative density of the alumina specimen sintered compare with single-step sintering at temperature of 1400°C for 0 and 1 h and two-step sintering at temperature of 1400°C for 0 h, 1150°C for 5 and 12 h with at heating rate of 10°C/min

4.7 Effect of HIP sintering process on the alumina sintered body

Generally, Hot Isostatic Press (HIP) is employed to reduce the size of pores within the grain and the grain boundaries so as to gain the fully dense specimen. The specimens treated in the HIP furnace should have the density higher than of 95% theoretical value. If the density of specimen prior to HIP stage was lower than 95% of theoretical, full density was not obtained after HIPing.

Therefore, the pre-sintered bodies with the relative density higher than 95% were selected to HIPing step to eliminate the residual pores in the samples. The condition of the HIP sintering was at temperature 1300°C for 2 h under 150 MPa in argon.

4.7.1 Density of the alumina HIP-sintered body

According to Figure 4.23 and 4.24, it was known that HIP process was a successful method to obtain the fully density both the effect of temperature and soaking time in pre-sintering.

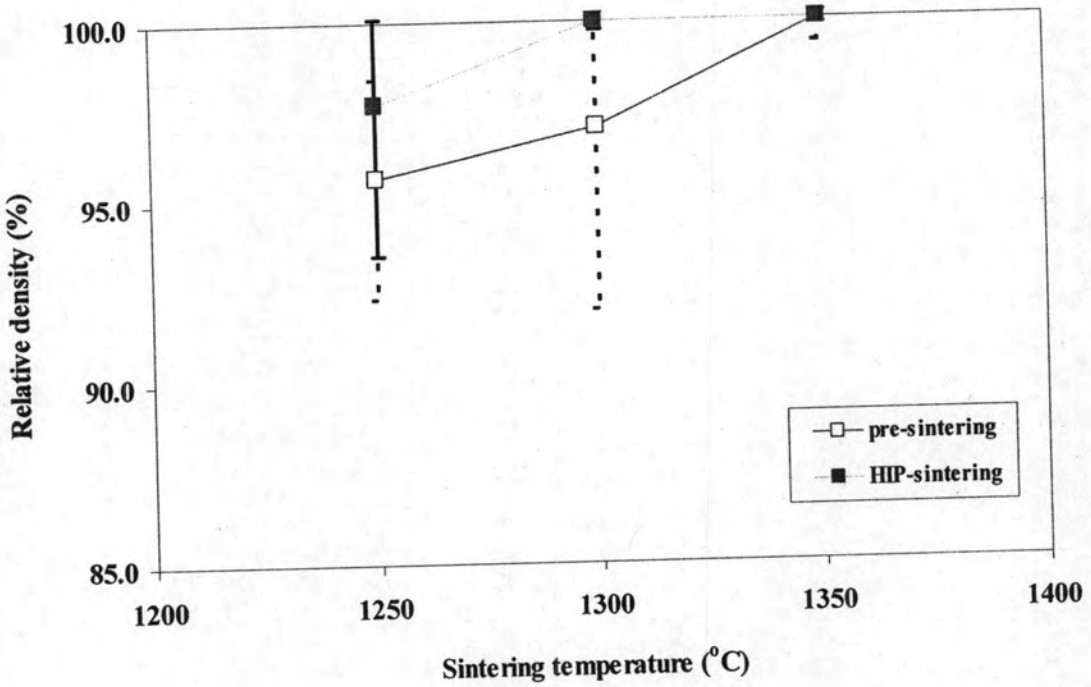

Figure 4.23 Relative density of alumina specimens with HIPing at temperature 1300°C for 2 h under 150 MPa in argon as different pre sintered temperature range of 1250 to 1350°C

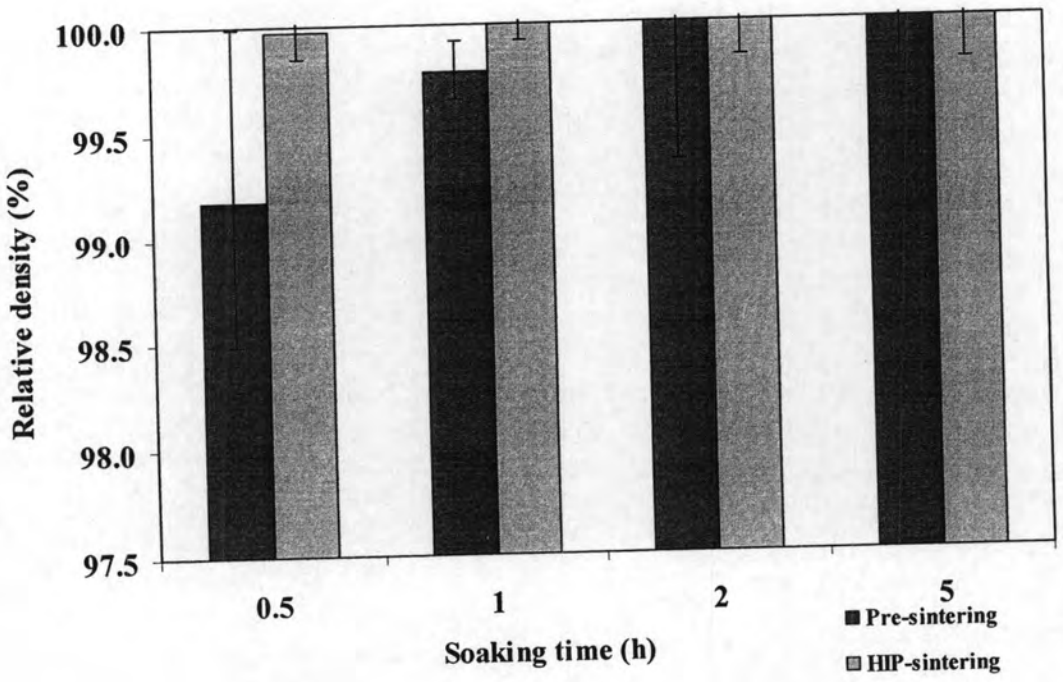

Figure 4.24 Relative density of alumina specimens with HIP sintered at temperature 1300°C for 2 h under 150 MPa in argon as different pre-sintered soaking time

4.7.2 Shrinkage of the alumina HIP-sintered body

As shown in Figure 4.25, the linear shrinkage of HIP-sintered body was lower than the pre-sintered body and decreased with high sintered temperature. It was demonstrated that the pre-sintered body became the densified specimen result in the low shrinkage of the HIPed body.

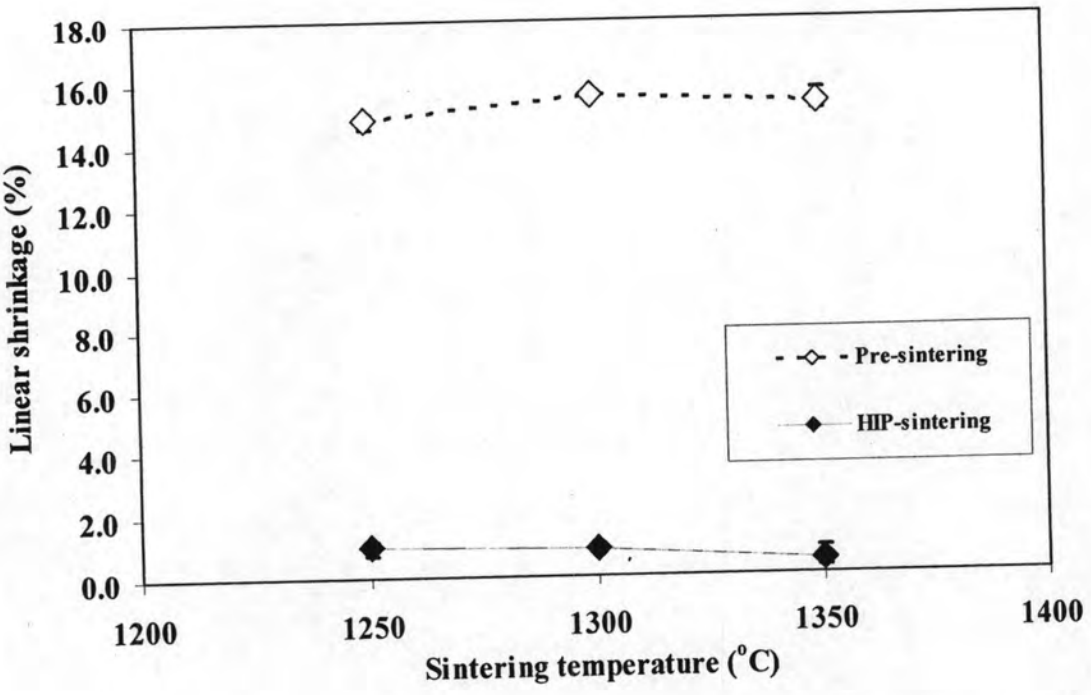

Figure 4.25 Linear shrinkage of specimens with HIP sintered at temperature 1300°C for 2 h under 150 MPa in argon as different pre-sintered temperature range of 1250 to 1350°C

4.7.3 Microstructure and average grain size of the alumina HIP-sintered body

As shown in Figures 4.26-4.29, the microstructure and grain size of HIPed bodies were characterized by AFM. The average grain size of HIPed body shown in Figure 4.26 was increased up to 0.2 μm in each pre sintered temperature that agrees with the microstructure in Figure 4.28. Corresponding to Figure 4.26, the average grain size of HIPed sample increased in the long soaking time and increased grain size of 0.2 μm from pre-sintered body. The microstructure of HIPed body with different soaking time was illustrated in Figure 4.29. It can be clearly seen that the grain growth occurred after HIP sintering.

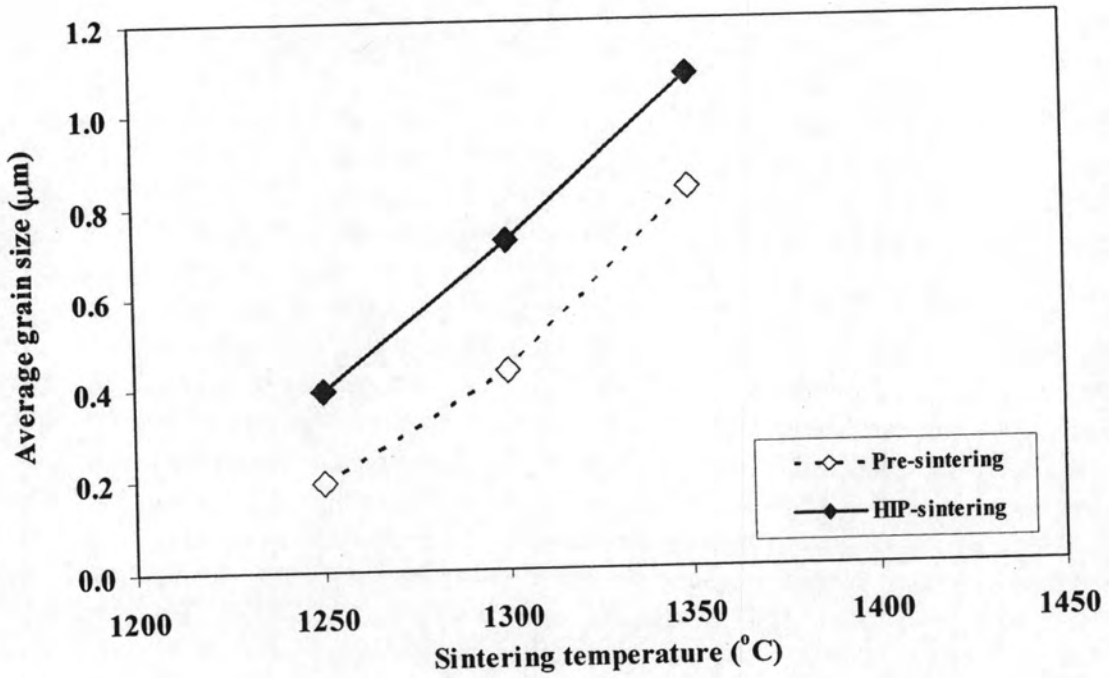

Figure 4.26 Grain size of specimens with HIP sintered at temperature 1300°C for 2 h under 150 MPa in argon as different pre-sintered soaking time range of 1250 to 1350°C

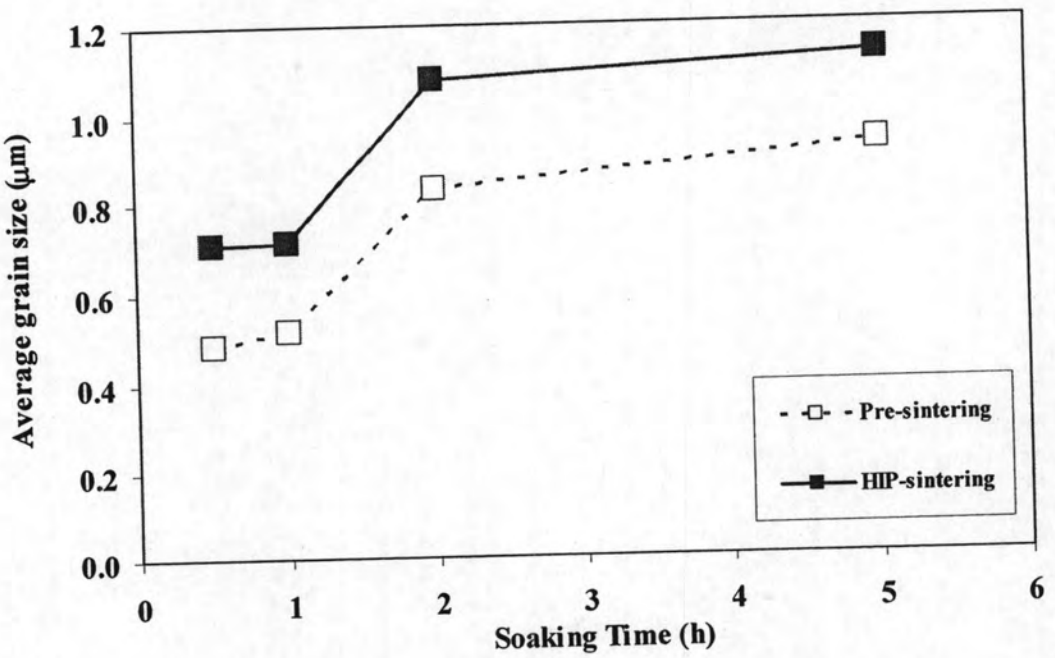

Figure 4.27 Grain size of specimens with HIP sintered at temperature 1300°C for 2 h under 150 MPa in argon as different pre-sintered soaking time

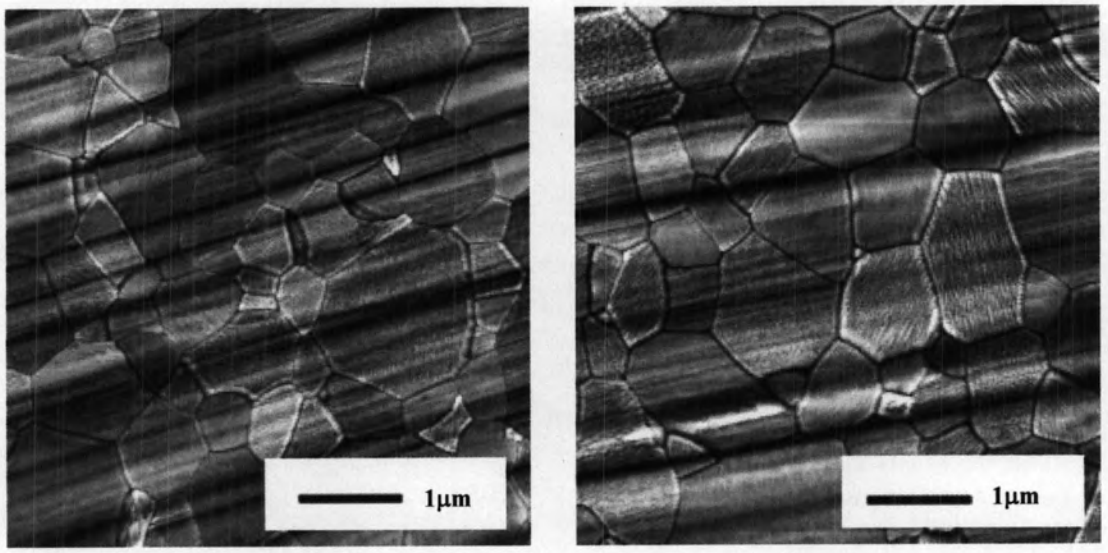

(a) (b)

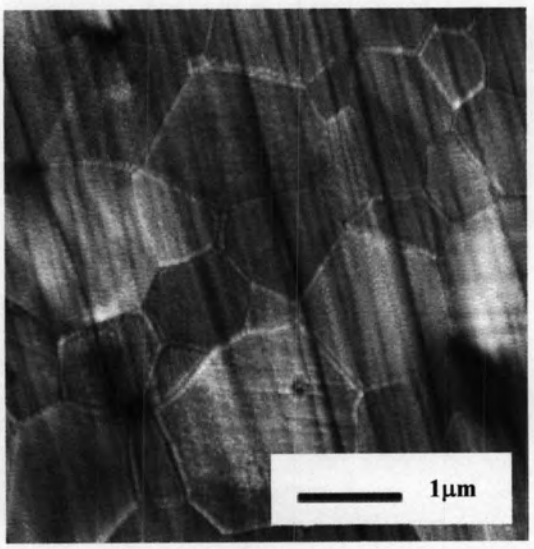

(c)

Figure 4.28 AFM micrograph of alumina specimens with HIP sintered at 1300°C, 150 MPa in argon atmosphere for 2 h and pre-sintering for 2 h at temperature of (a) 1250°C (b) 1300°C (c) 1350°C

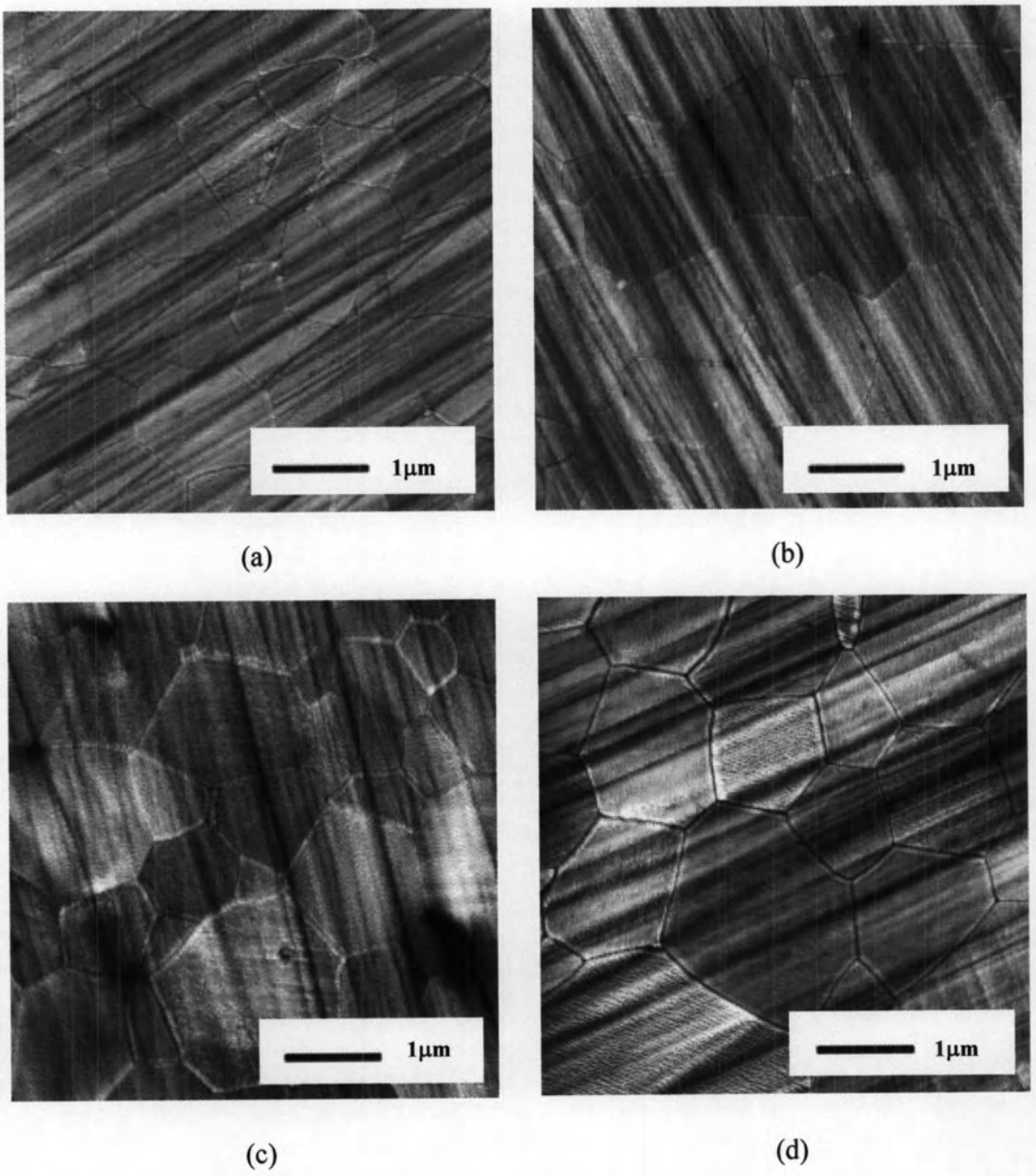

Figure 4.29 AFM micrograph of alumina specimens with HIP sintered at 1300°C, 150 MPa in argon atmosphere for 2 h and pre-sintering at temperature of 1350°C for (a) 0.5 h (b) 1 h (c) 2 h (d) 5 h

4.7.4 Appearance of the alumina HIP-sintered body

The appearance of sintered specimen before and after HIP sintering was exhibited in Figure 4.30. The color of alumina HIPed bodies changed from white to gray specimen. When HIPed specimens were ground to 0.8 mm, it became to transparency as illustrated in Figure 4.31.

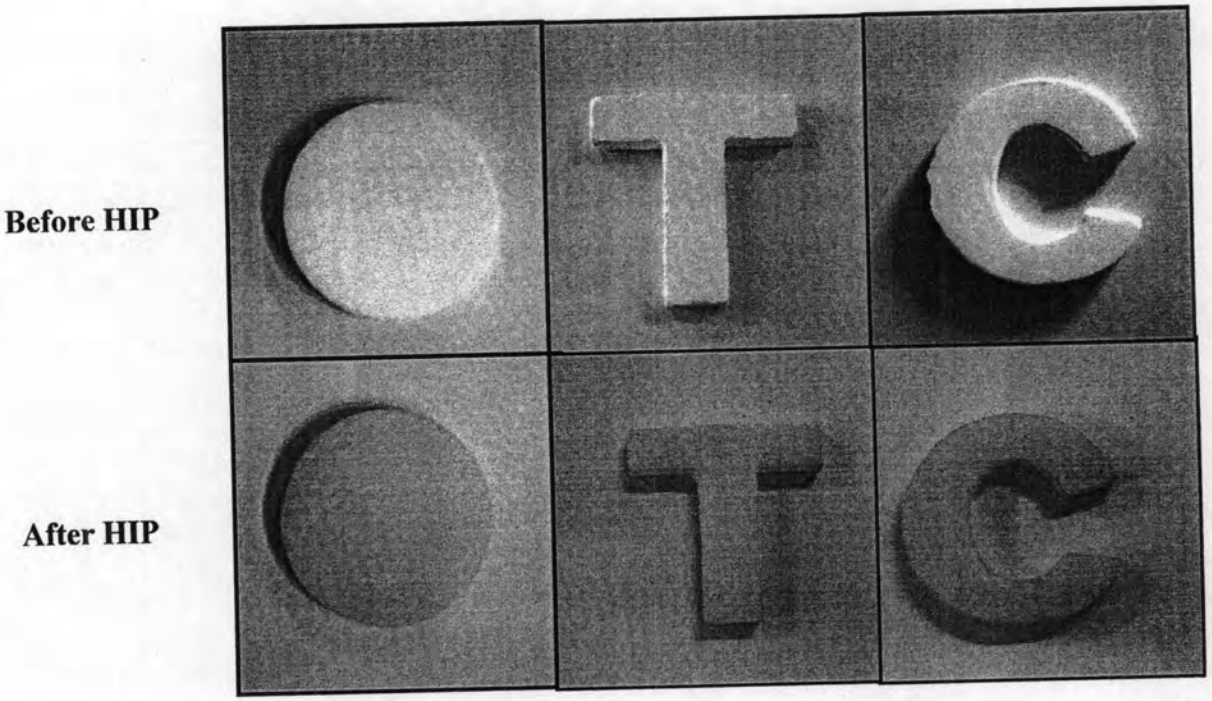

Figure 4.30 The alumina sintered bodies in various shapes as (a) before HIP and (b) after HIP at 1300°C 150 MPa in argon atmosphere

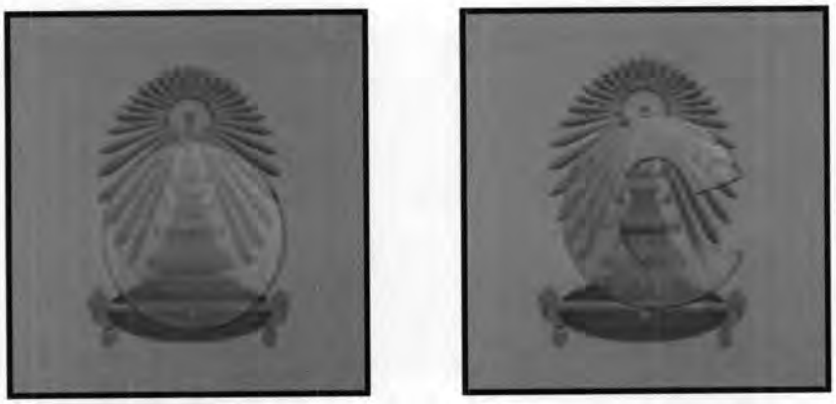

(a) (b)

Figure 4.31 HIPed specimens that pre-sintered in atmosphere and followed by HIPing at 1300°C, 150MPa in argon atmosphere for 2 h after grinding to 0.8 mm thickness (a) circular pellet shape with pre-sintered at 1250°C for 2 h (b) C shape with pre-sintered at 1300°C for 2 h

4.7.5 Transmittance of the alumina HIP-sintered body

The HIPed specimens with full density and tendency to exhibit transparency were selected to grind for reducing their thickness to 0.8 mm. These specimens were characterized the transmittance (%) by UV-VIS spectrophotometer at wavelength of 200-900 nm. As shown in Figures 4.32 and 4.33, the transmittance of HIPed specimens was dependent on the value of wavelength and grain size, respectively. The transmittance increased with the increasing wavelength. The maximum transmittance at wavelength of 900 nm was 81.87, 74.78, 72.95, 71.91 and 68.74% with samples of A1, B1, A3, B2 and A2, respectively. Moreover, the appearance of HIPed specimens measured the transmittance was illustrated in Figure 4.34. It was reasonable that the HIPed specimen with pre-sintering at 1250°C for 2 h had the highest transmittance, leading to the grain size as a submicron scale of 0.393 μm. The relation between transmittance and grain size of HIPed specimen at the different pre-sintering conditions was shown in Figure 4.33. It was known that the transmittance decreased with the increasing grain size. In accordance with the model for grain boundary scattering at zero porosity based on the Rayleigh-Gans-Debye

theory, the real in-line transmittance was an inverse proportion with the grain size (Apetz, et al., 2003).

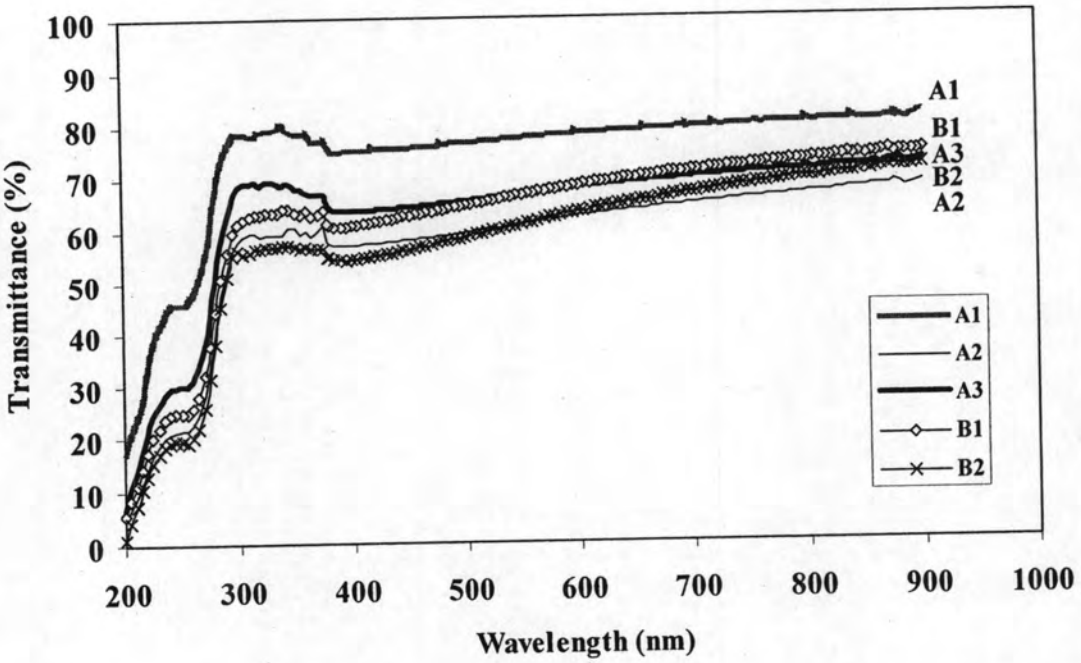

Figure 4.32 Transmittance of HIPed specimens in range of 200-900 nm with thickness of 0.8 mm as the different pre-sintering

Table 4.2 Code of alumina specimens with the pre-sintered and followed the HIP

Code	Pre sintering condition*
A1	One-step: 1250°C for 2 h
A2	One-step: 1300°C for 2 h
A3	One-step: 1350°C for 1 h
B1	Two-step: 1400°C for 0 h, 1150°C for 5 h
B2	Two-step: 1400°C for 0 h, 1150°C for 12 h

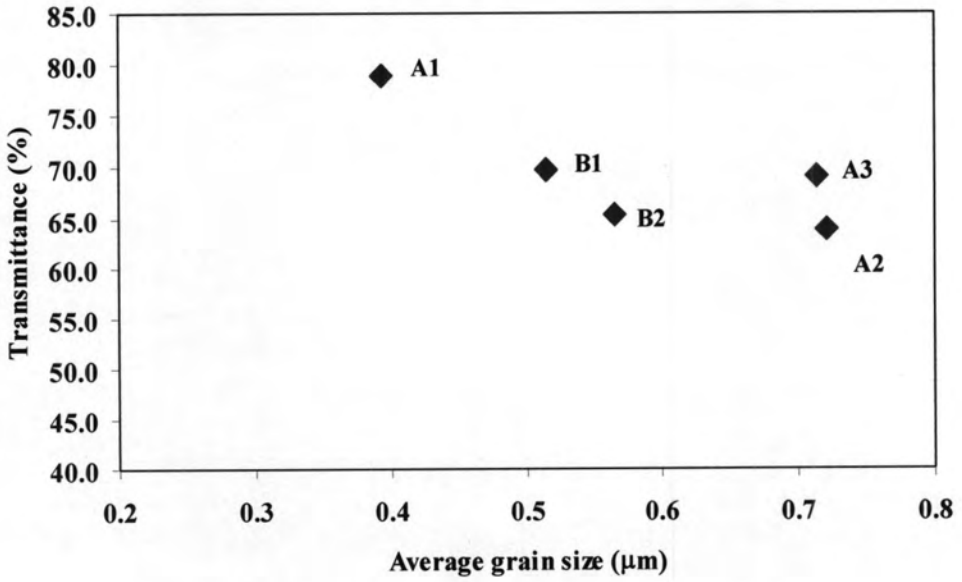

Figure 4.33 Transmittance of HIPed specimens at wavelength of 645 nm as a function of average grain size

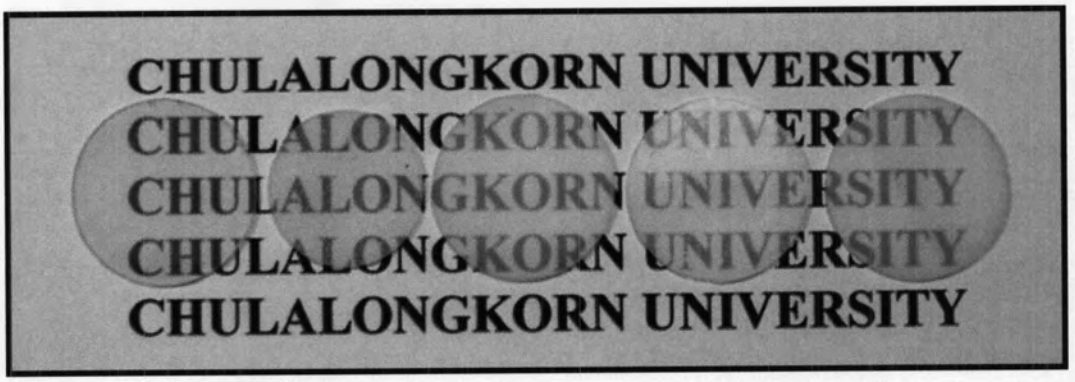

Figure 4.34 The appearance of the HIP specimens measured the transmittance as A1, B1, A3, B2 and A2 ordered the left side to the right side

Based on the experimental results in the transmittance of HIPed specimens, the alumina sample with full density and submicron grain size could exhibit the fairly good transparent property of the polycrystalline alumina. Furthermore, the acid treatment of calcined body before sintering could provide improved transparency of HIPed body as also reported by Areeraksakul (2005). The treated specimen exhibited better transmittance than that of untreated. This is attributable to the reason that the specimens without acid treatment had much amount of grains with smaller than average compare with acid treatment specimens.